

# Supporting information for

## One Hour Road to High-Quality Arrays of Gold Nanoparticles Coated with Organic Ligand

*Thibault Degoussée, William G. Neal, Zach Edwards, Saumya Singh, Jotham Selvarajah, Teymour Talha-Dean, Bob C. Schroeder, Matteo Palma, Jan Mol*

Figure S1: Picture of aqueous colloidal AuNP synthesized in different vials.

Figure S2: Resistance of AuNP-C12 made by 3pD with  $n=1$ .

Figure S3: Morphology of the 3pD monolayers.

Figure S4: IV traces of 3pD arrays

Figure S5: UV-Vis spectroscopy of AuNP-Ligand in solution and solid state.

Figure S6: IV curves of monolayers formed on a convex water surface.

Figure S7: AFM analysis of the monolayers formed on a convex water surface.

Figure S8: TEM analysis of the monolayers formed on a convex water surface.

Page 10: Synthesis route of 3-(7-(2-(octyldisulfaneyl)ethyl)-1,3,6,8-tetraoxo-3,6,7,8-tetrahydrobenzo[Imn][3,8] phenanthroline-2(1H)-yl)propanoic acid.

Figure S9: Synthesis,  $^1\text{H-NMR}$ , and  $^{13}\text{C-NMR}$  spectrum of compound 4: tert-butyl (2-(octyldisulfaneyl)ethyl)carbamate.

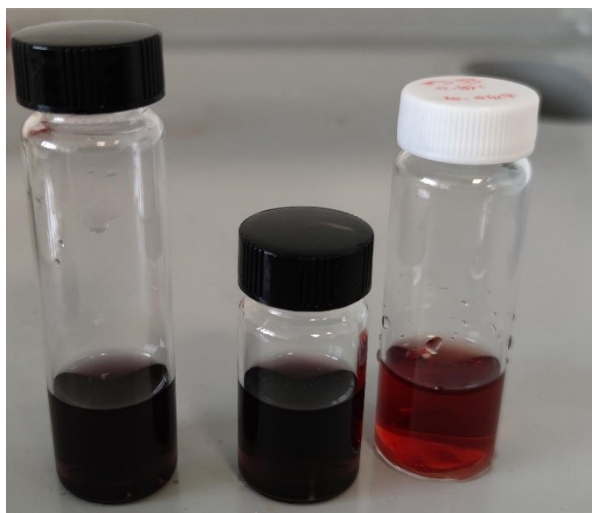
Figure S10: Synthesis,  $^1\text{H-NMR}$ , and  $^{13}\text{C-NMR}$  spectrum of compound 5: 2-(octyldisulfaneyl)ethan-1-amine.

Figure S11: Synthesis,  $^1\text{H-NMR}$ , and  $^{13}\text{C-NMR}$  spectrum of compound 7: 3-(7-(2-(octyldisulfaneyl)ethyl)-1,3,6,8-tetraoxo-3,6,7,8-tetrahydrobenzo[Imn][3,8] phenanthroline-2(1H)-yl)propanoic acid.

Figure S12: Solid phase exchange of C12 with 3-(7-(2-(octyldisulfaneyl)ethyl)-1,3,6,8-tetraoxo-3,6,7,8-tetrahydrobenzo[Imn][3,8] phenanthroline-2(1H)-yl)propanoic acid.

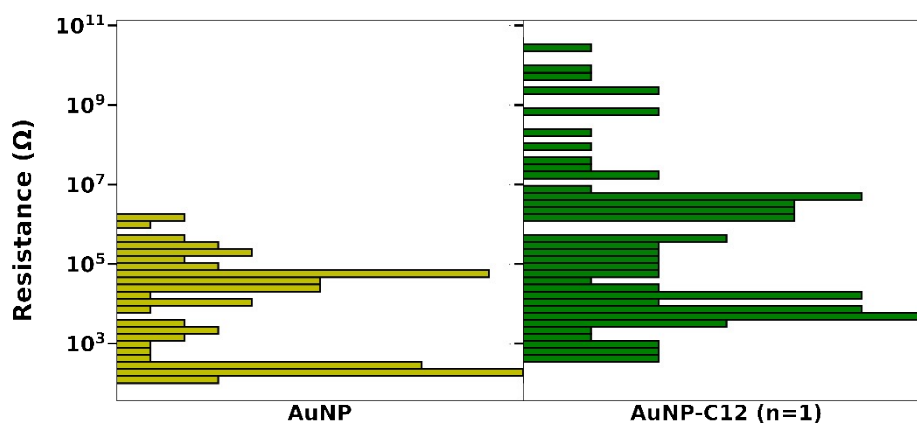
Figure S13: Comparison of  $^1\text{H-NMR}$  spectra of 7 and AuNP-7.

**Figure S1: Picture of aqueous colloidal AuNP synthesized in different vials**



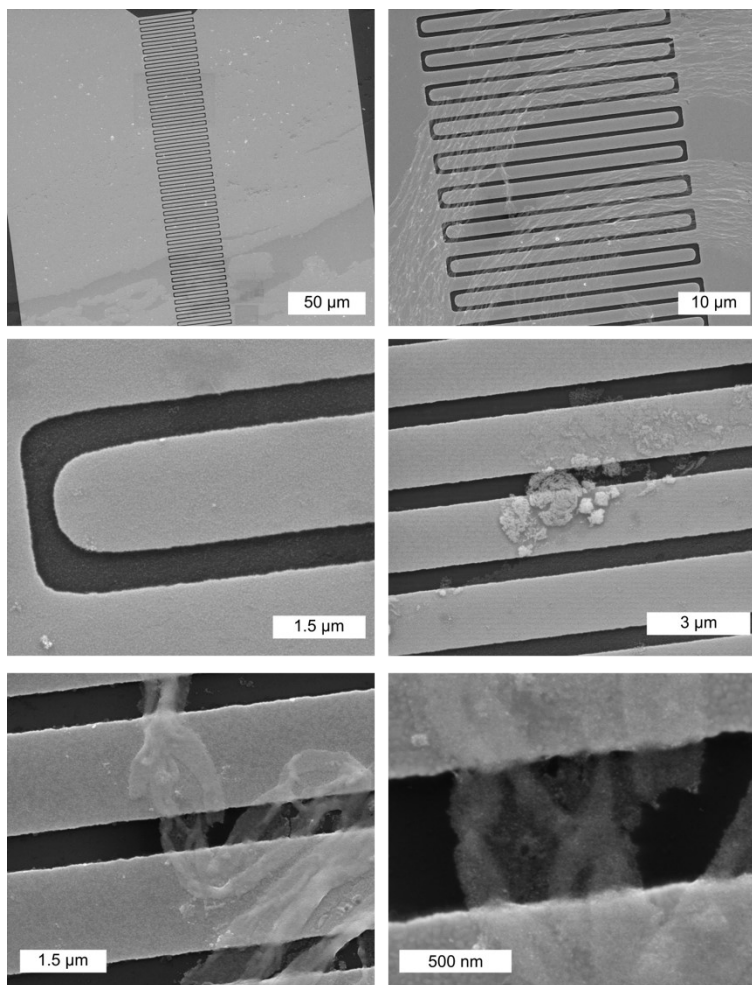
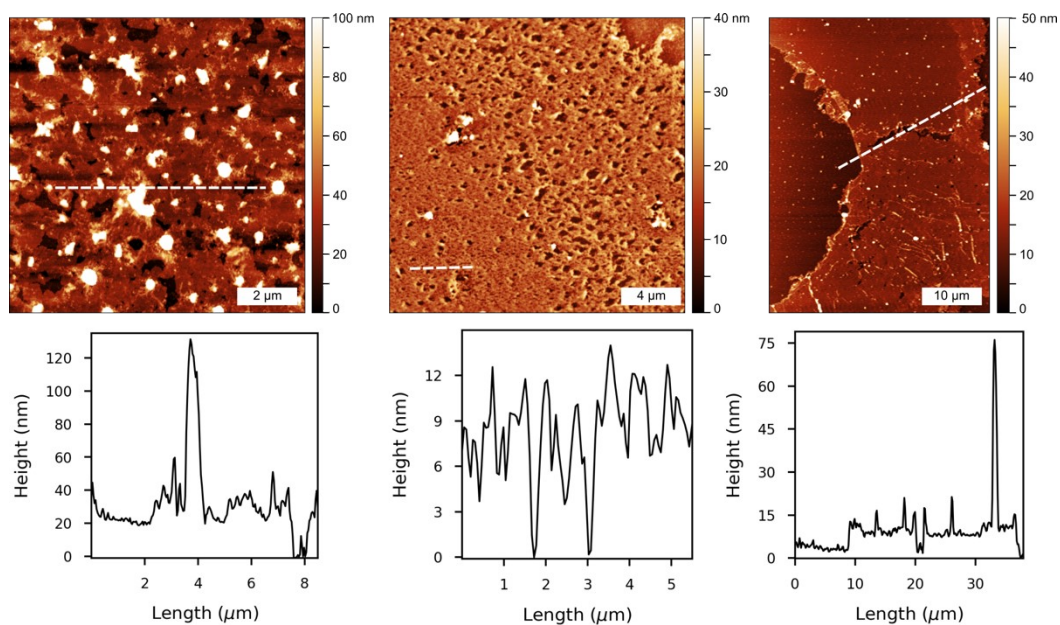
These three solutions were made within 10 minutes using the same stock solutions of  $\text{H AuCl(III)}$  in  $\text{HCl}$  and  $\text{NaBH}_4$  in  $\text{NaOH}$ . Vials with a black lid are borosilicate glass and the vial with a white lid is soda-lime glass.

Figure S2: Resistance of AuNP-C12 made by 3pD with n=1



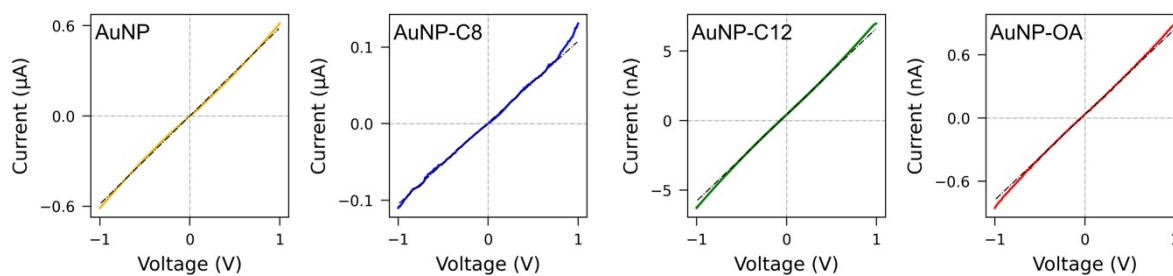
The concentration of ligand is an important parameter in the three-phase monolayer formation method. With the diameter of the AuNP nanoparticles, the theoretical concentration of ligand needed to completely coat all the AuNP in 1 mL, ' $n$ ', can be calculated (see main text). The yellow distribution represents the resistance of 80 devices covered with a monolayer of AuNP not linked by any molecule, which is around  $\sim 10^2$ - $10^5$  Ω. The green distribution represents the resistance measured of 80 devices covered with a monolayer of AuNP-C12 made with the theoretical concentration. Both distributions are alike which indicate that this n=1 concentration is not enough to coat the AuNP with a ligand.

Figure S3: AFM analysis of the 3pD monolayers



SEM images of the IDE electrodes (top), a set of electrodes with a clean coverage (middle left) or with aggregates and partial coverage of the electrodes (middle right and bottom).

**Figure S4: IV traces of 3pD arrays.**



This figure shows the IV traces of 3pD layers with the highest resistances. All devices show an Ohmic behaviour and the resistance increases as we increases the length of the ligand.

Figure S5: UV-Vis spectroscopy of AuNP-Ligand in solutions and solid state

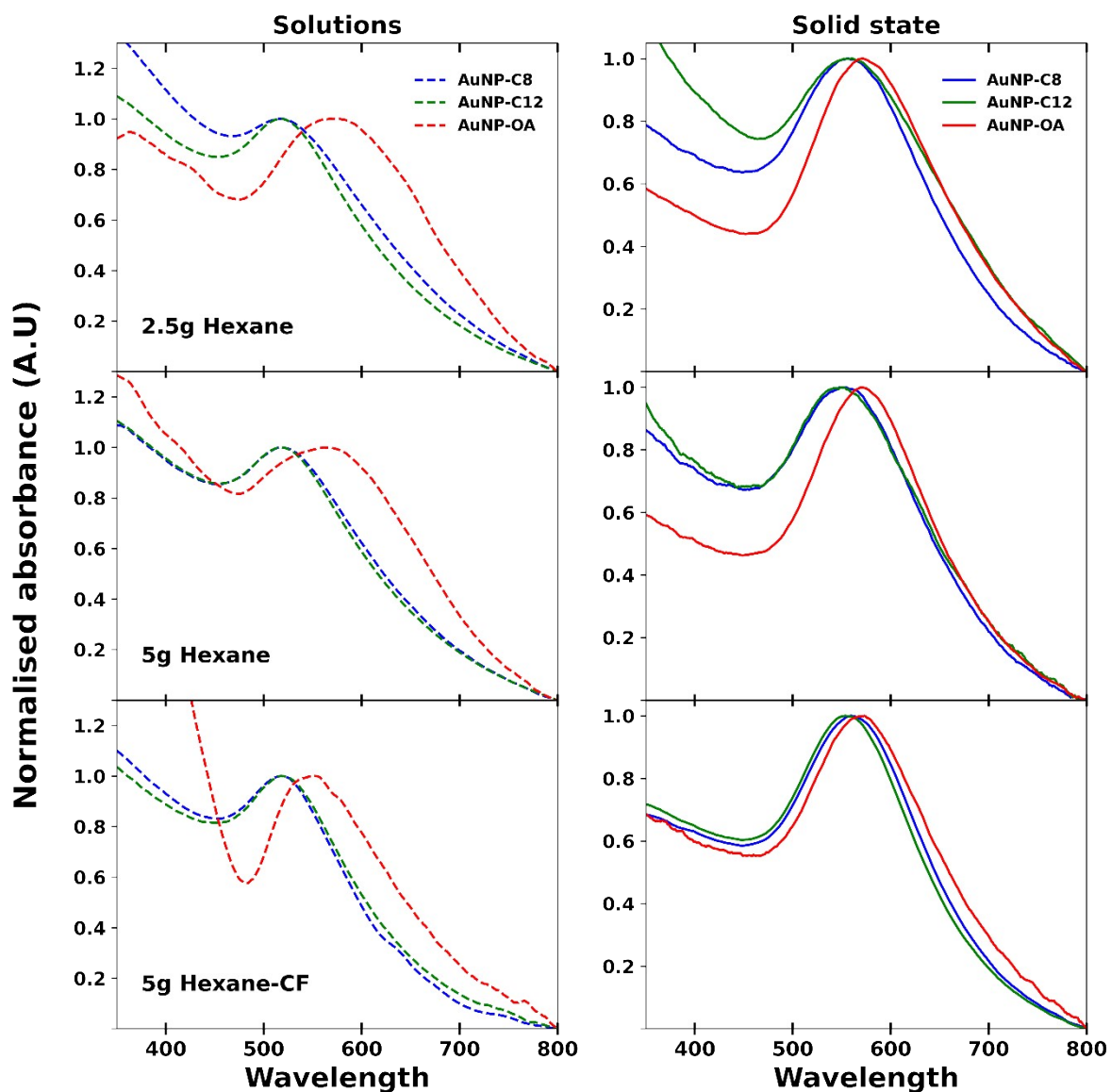
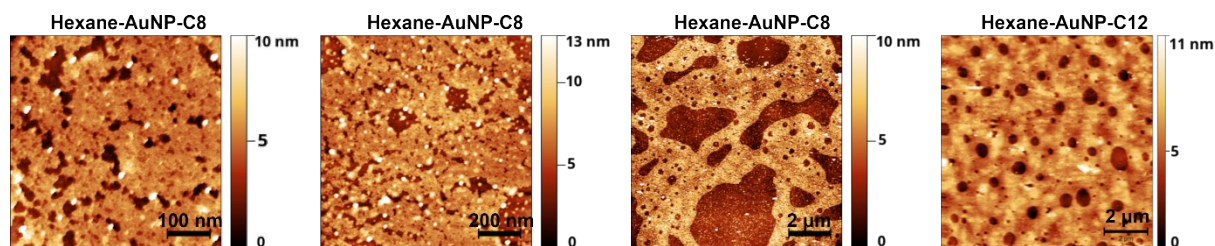
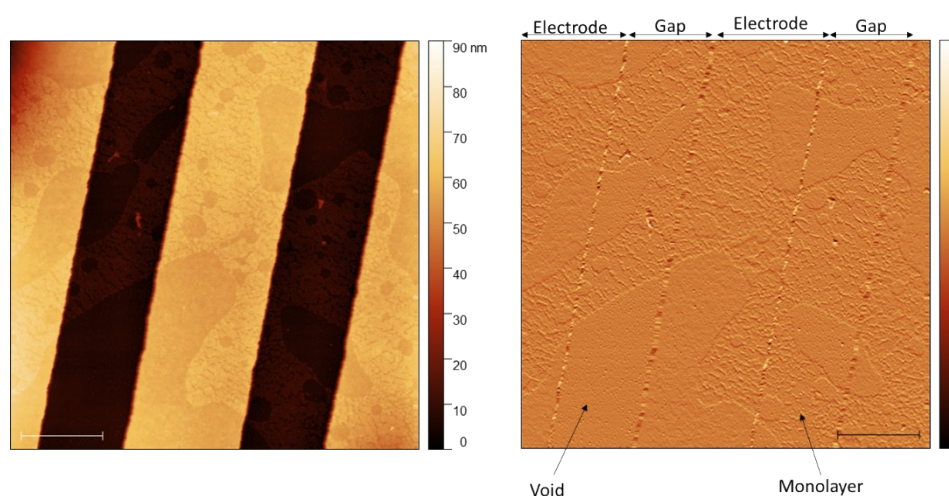


Figure S6: AFM analysis of the monolayers formed on a convex water surface

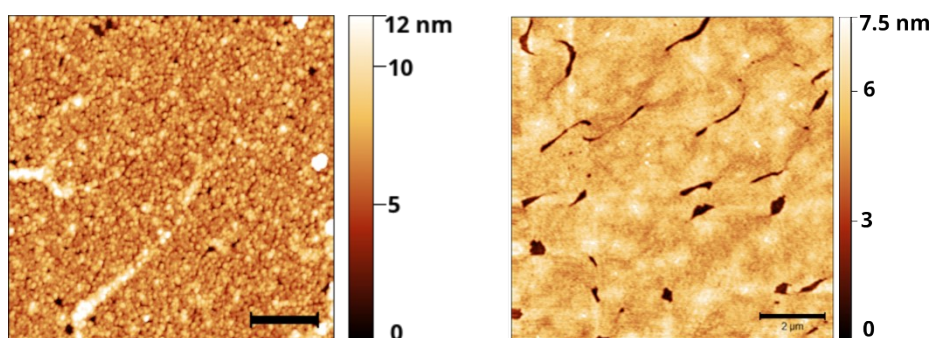
**Hexane-AuNP:**



The first three columns are topographies of hexane-AuNP-C8 network. From left to right, the scan dimensions (scale bar) are 0.5 x 0.5 μm (100 nm), 1 x 1 μm (200 nm) and 10 x 10 μm (2 μm). The last column is a 10 x 10 μm (2 μm ) topography of the hexane-AuNP-C12 monolayer.



We imaged a set of interdigitated electrodes (IDE) on a device for hexane-AuNP-C8 network. The picture on the left shows the as measured image while on the right, we modified the picture to show the network spreading across the IDE. The dimensions are 5 x 5 μm and the scale bars are 1 μm. Although network formed from a pure hexane phase have a lot of voids, the network is long enough to cover several micrometres.

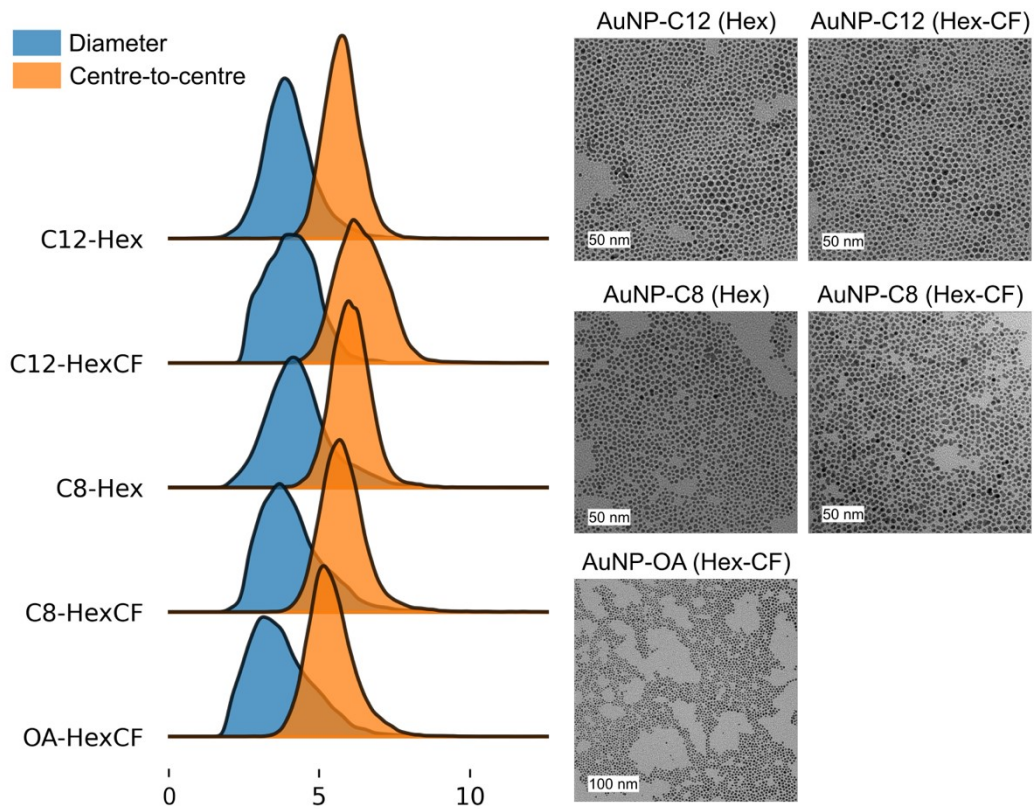


**Hexane-CF-AuNP:**

On the left is a 1 x 1 μm (200 nm) image of hexane-chloroform-AuNP-C8 which show almost perfect coverage of the whole surface. On the right is a 10 x 10 μm (2 μm) image of hexane-CF-AuNP-C12 monolayer which also show an almost perfect coverage with less defects.

**Figure S7: TEM analysis of AuNP-Ligand monolayers formed on a convex water surface.**

Distribution of the AuNP diameter and centre-to-centre distances for different AuNP-ligand monolayers. The difference between the centre-to-centre and the diameter corresponds to



the length of the ligand (below).

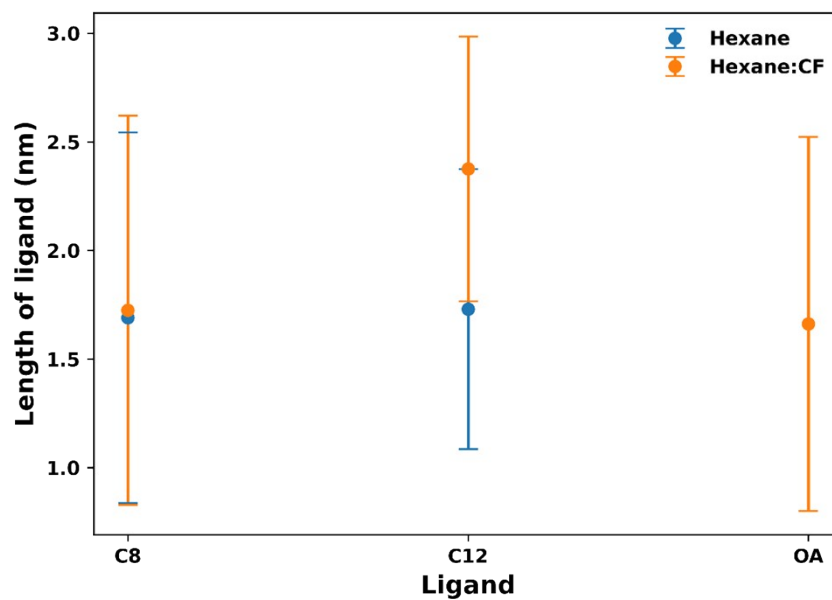
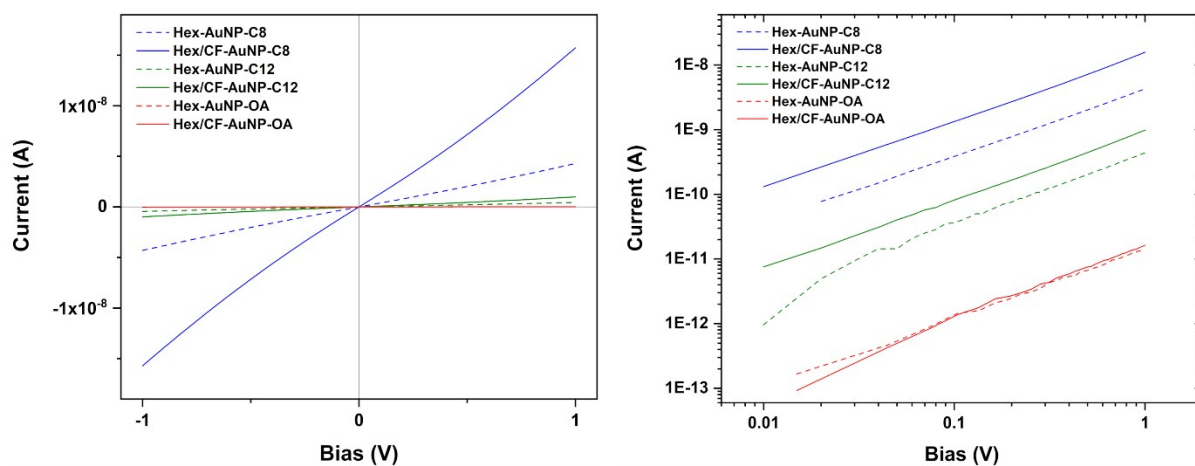




Figure S8: IV curves of monolayers formed on a convex water surface



IV curves of the different AuNP-linker made either from pure hexane or a mixture of hexane-chloroform. The double logarithmic plot shows the linear  $I \propto V$  dependence of all networks at room temperature and between  $\pm 1V$ .

## General Experimental

All reagents and solvents used were obtained from commercial suppliers and used without further purification. Di-*tert*-butyl (disulfaneyldiylbis(ethane-2,1-diyl))dicarbamate (**2**) and *tert*-butyl (2-mercaptoethyl)carbamate (**3**) were synthesized according to a previously published procedure.<sup>1</sup> Reactions were carried out under nitrogen atmosphere using standard Schlenk techniques and reported yields refer to purified and spectroscopically pure compounds, unless otherwise stated. Concentration under reduced pressure was performed by rotary evaporation (25 - 40 °C) at an appropriate pressure. Thin layer chromatography (TLC) was performed using Merck Si60 F254 pre-coated TLC aluminium plates and flash column chromatography was performed using Merck Geduran Si 60 silica gel (40–63 μm particle size). <sup>1</sup>H and <sup>13</sup>C nuclear magnetic resonance (NMR) spectra were recorded on Bruker NMR spectrometers *Avance III 400* and *Avance Neo 700* at 298 K. Chemical shifts (δ) are reported in parts per million (ppm), using the residual solvent peaks as internal standard. For <sup>1</sup>H-NMR (δ): CDCl<sub>3</sub> 7.26, DMSO-*d*<sub>6</sub> 2.50. For <sup>13</sup>C-NMR (δ): CDCl<sub>3</sub> 77.16, DMSO-*d*<sub>6</sub> 39.52. Coupling constants (*J*) are given in Hertz (Hz) and spin multiplicities denoted as follows: s = singlet, bs = broad singlet, d = doublet, p = pentet. Mass spectrometry data was collected on a *Thermo Accela LC/LTQ* (EI), *Waters LCT Premier QTOF* (ESI) and *Thermo Scientific TRACE 1310 GC* (EI/CI) mass spectrometers (ESI). Fourier-transform infrared spectra (FTIR) were recorded on a *Bruker Platinum ATR* with a single reflection diamond attachment.

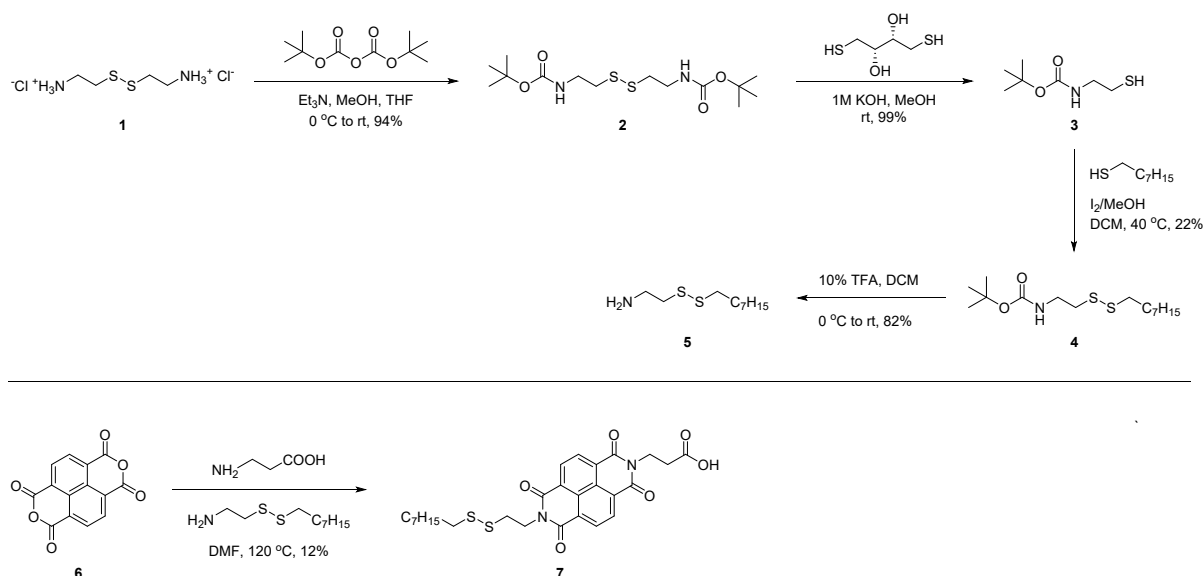
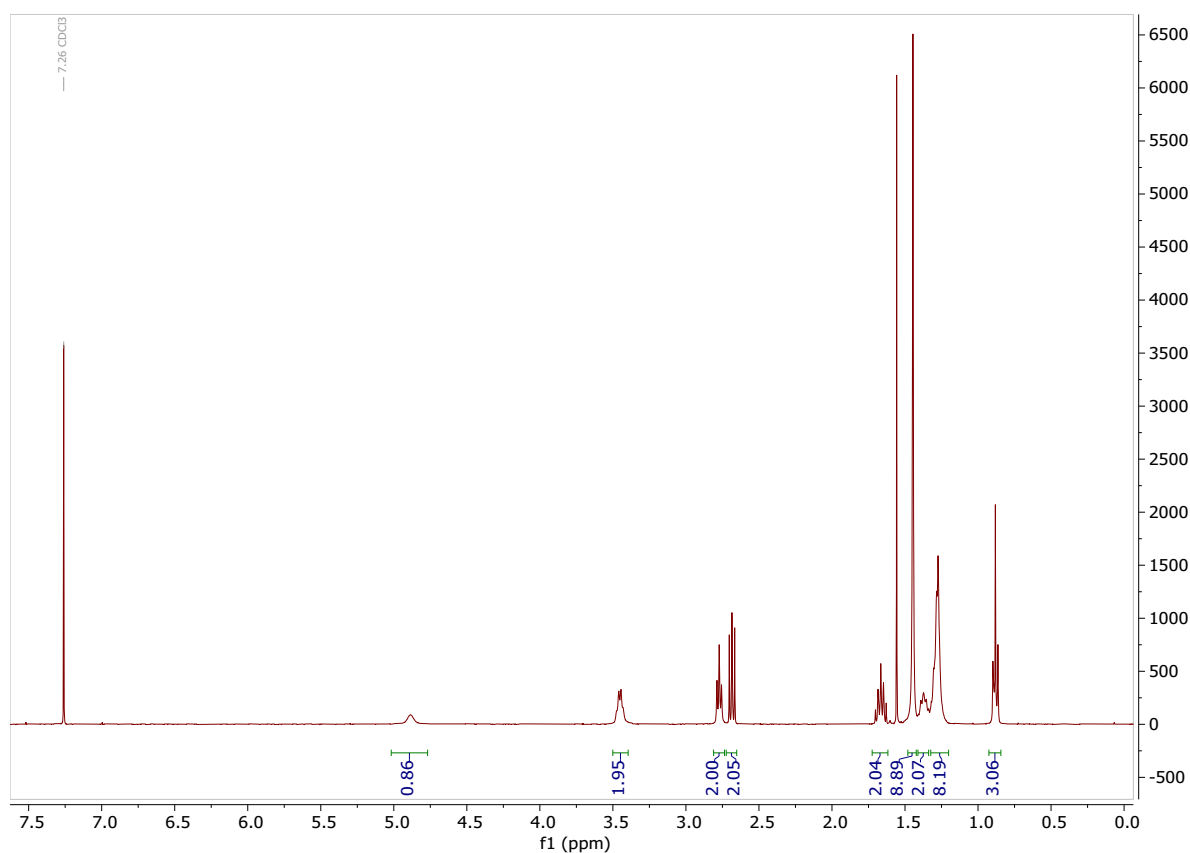


**Figure S9: Synthesis, <sup>1</sup>H-NMR, and <sup>13</sup>C-NMR spectrum of compound 4: *tert*-butyl (2-(octyldisulfaneyl)ethyl)carbamate**

The synthesis of *tert*-butyl (2-(octyldisulfaneyl)ethyl)carbamate (**4**) was performed by modifying the procedure of Cheng and Miller.<sup>2</sup> Octane-1-thiol (3.91 g, 26.7 mmol) and *tert*-butyl (2-mercaptoethyl)carbamate (**3**) (4.74 g, 26.7 mmol) were dissolved in 300 mL of DCM and heated to 40 °C. Iodine (5.00 g, 19.7 mmol) dissolved in MeOH (50 mL) was added slowly until the reaction mixture remained pale yellow. The solution was cooled down and the solvents removed in vacuo. The resulting crude product was purified by flash column chromatographic using 40% of DCM in hexane with addition of 1% methanol as eluent. The target compound **4** (1.90 g, 5.91 mmol, 22%) was recovered as a pale yellow oil. <sup>1</sup>H NMR (400 MHz, CDCl<sub>3</sub>) δ 4.89 (bs, 1H), 3.50 – 3.40 (m, 2H), 2.77 (t, *J* = 6.2 Hz, 2H), 2.71 – 2.66 (m, 2H), 1.72 – 1.62 (m, 2H), 1.45 (s, 9H), 1.41 – 1.34 (m, 2H), 1.32 – 1.23 (m, 8H), 0.88 (t, *J* = 6.8 Hz, 3H). <sup>13</sup>C NMR (101 MHz, CDCl<sub>3</sub>) δ 155.83, 79.53, 39.31, 39.12, 38.45, 31.88, 29.27, 29.25, 28.61, 28.49, 22.73, 14.19. HRMS (ESI) calcd. for C<sub>15</sub>H<sub>32</sub>NO<sub>2</sub>S<sub>2</sub> [M+H]<sup>+</sup> 322.1874; obs. 322.1872.

<sup>1</sup>H-NMR spectrum of compound 4.



$^{13}\text{C}$ -NMR spectrum of compound 4.

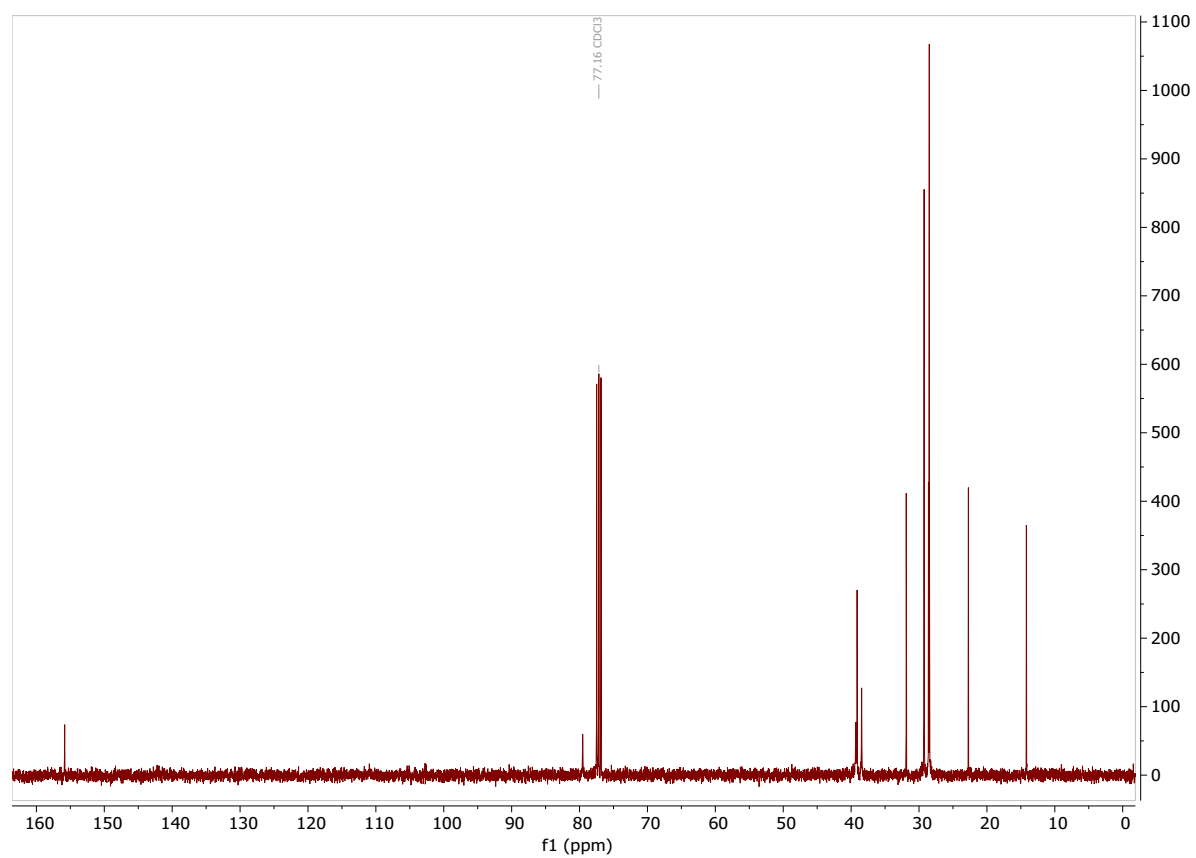
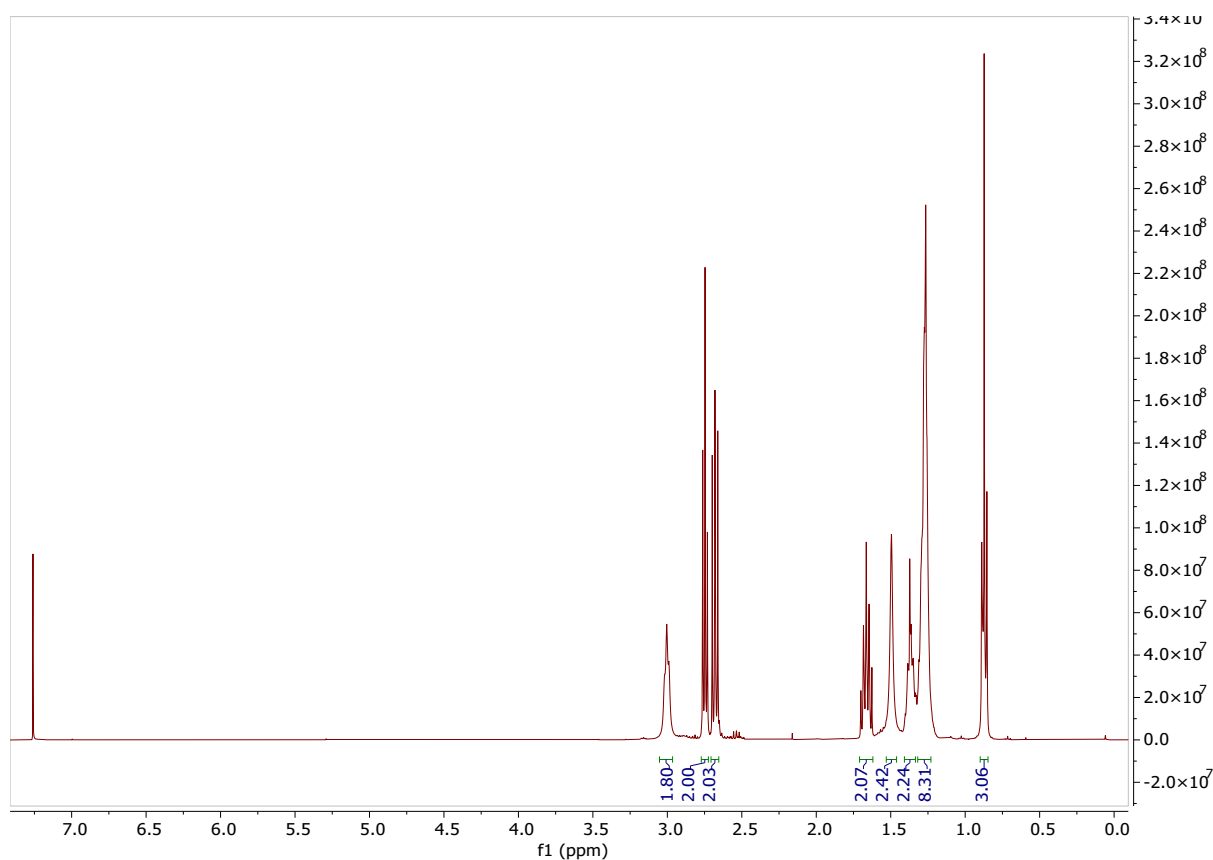


**Figure S10: Synthesis,  $^1\text{H}$ -NMR, and  $^{13}\text{C}$ -NMR spectrum of compound 5: 2-(octyldisulfaneyl)ethan-1-amine**

The conditions for the deprotection of **4** were adapted from a previous report.<sup>3</sup> Anhydrous dichloromethane (20 mL) containing 10% of trifluoroacetic acid (2 mL) was cooled to 0 °C with an ice bath, before *tert*-butyl (2-(octyldisulfaneyl)ethyl)carbamate (**4**) (1.50 g, 4.67 mmol) was added. The ice-bath was removed and the reaction warmed to room temperature and stirred for an additional 6 hours. The reaction was neutralised by the addition of saturated  $\text{NaHCO}_3$  solution and the organic layer separated. The organic layer was washed with brine and dried over  $\text{MgSO}_4$ . After filtration the solvent was evaporated and the crude product purified by flash column chromatography using DCM with 5% MeOH as eluent, yielding the desired product **5** (0.85 g, 3.84 mmol, 82%).  $^1\text{H}$  NMR (400 MHz,  $\text{CDCl}_3$ )  $\delta$  3.01 (t,  $J = 6.2$  Hz, 2H), 2.75 (t,  $J = 6.2$  Hz, 2H), 2.69 (t,  $J = 7.5$  Hz, 2H), 1.67 (p,  $J = 7.3$  Hz, 2H), 1.44 (bs, 2H), 1.33 – 1.23 (m, 8H), 0.88 (t,  $J = 7.1, 6.6$  Hz, 3H).  $^{13}\text{C}$  NMR (101 MHz,  $\text{CDCl}_3$ )  $\delta$  42.72, 40.74, 39.27, 31.91, 29.30, 29.28, 28.65, 22.76, 14.21. HRMS (ESI) calcd. for  $\text{C}_{10}\text{H}_{23}\text{NS}_2$   $[\text{M}+\text{H}]^+$  222.1350; obs. 222.1349.

$^1\text{H}$ -NMR spectrum of compound 5.



$^{13}\text{C}$ -NMR spectrum of compound 5.

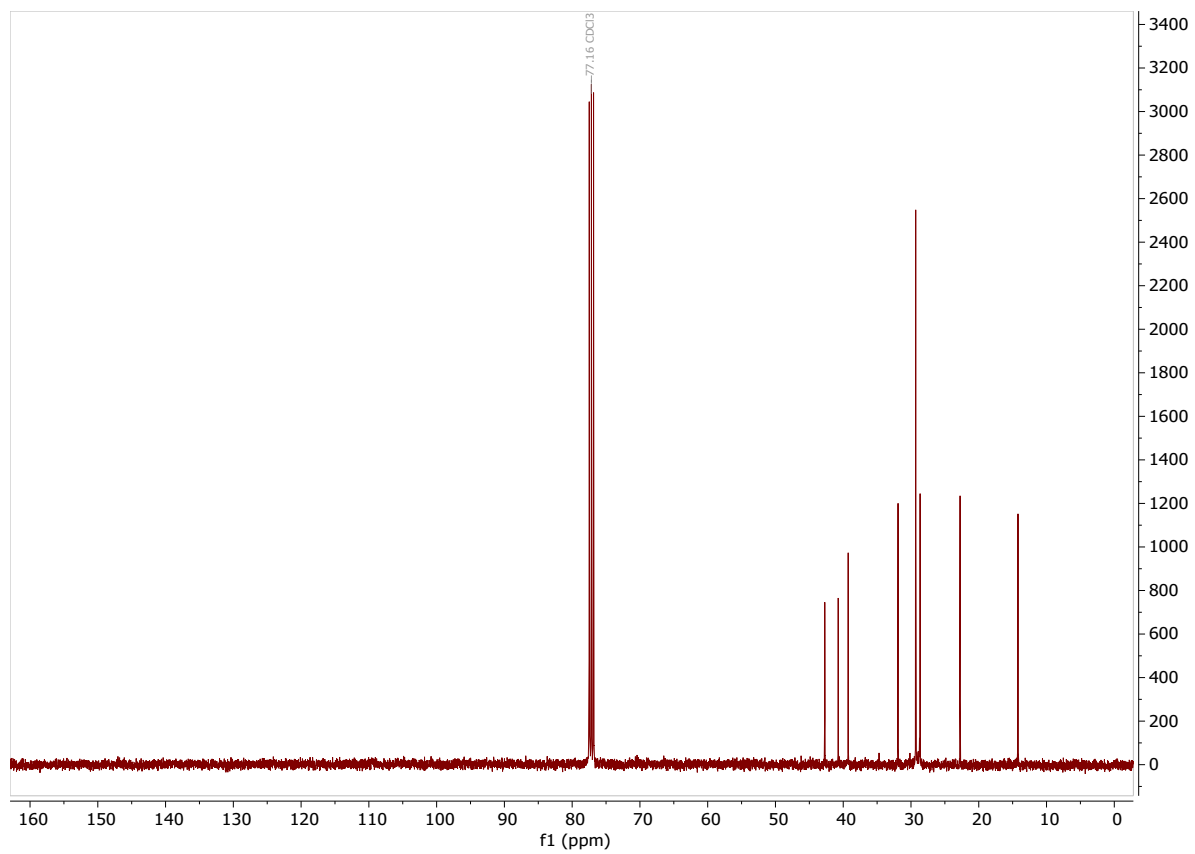
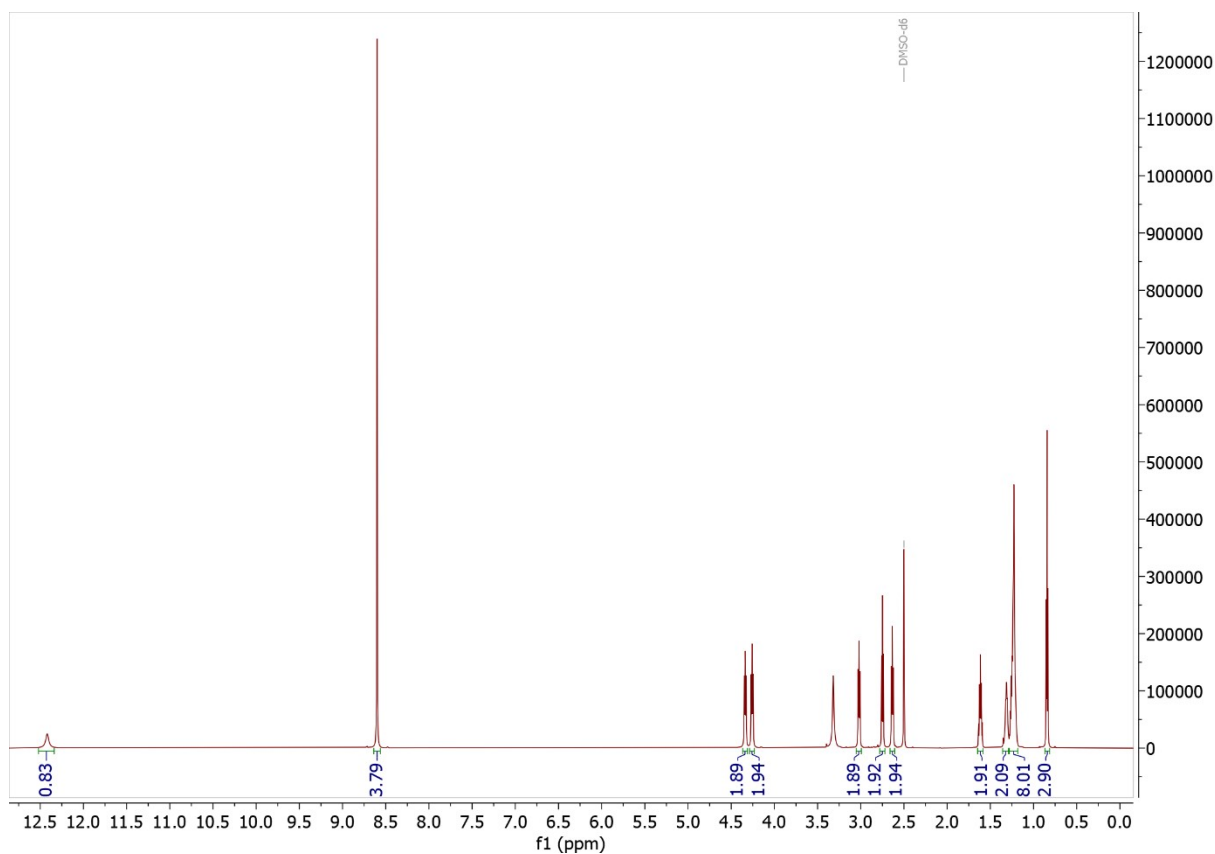


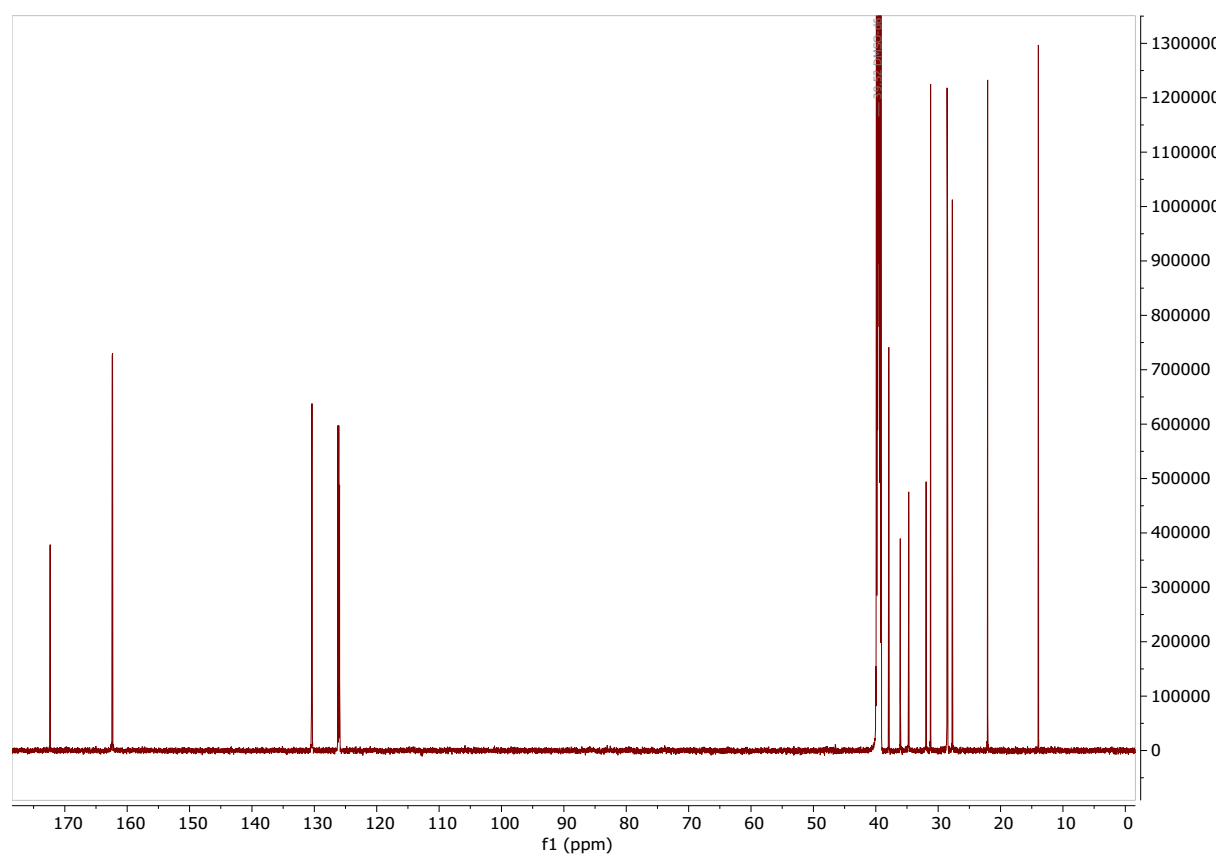
**Figure S11: Synthesis,  $^1\text{H}$ -NMR, and  $^{13}\text{C}$ -NMR spectrum of compound 7: 3-(7-(2-(octyldisulfaneyl)ethyl)-1,3,6,8-tetraoxo-3,6,7,8-tetrahydrobenzo[*lmn*][3,8]phenanthrolin-2(1*H*)-yl)propanoic acid**

1,4,5,8 Naphthalene-tetracarboxylic dianhydride (**6**) (600 mg, 2.24 mmol),  $\beta$ -alanine (199 mg, 2.24 mmol) and 2-(octyldisulfaneyl)ethan-1-amine (**5**) (495 mg, 2.24 mmol) was dissolved in 10 mL of anhydrous DMF and the resulting suspension was stirred for 12 hours at 130 °C. After cooling to room temperature, the reaction mixture was placed in the refrigerator for 30 minutes to allow the product to precipitate from the solution. The precipitate was filtered off and washed with MeOH several times. The recovered crude product was further purified by column chromatography using silica gel as stationary phase and 3-5% MeOH in  $\text{CHCl}_3$  as eluent to afford the target product **7** as light-yellow solid (150 mg, 276  $\mu\text{mol}$ , 12%).  $^1\text{H}$  NMR (700 MHz,  $\text{DMSO-}d_6$ )  $\delta$  12.42 (bs, 1H), 8.60 (s, 4H), 4.34 (t,  $J = 7.3$  Hz, 2H), 4.26 (t,  $J = 7.9$  Hz, 2H), 3.02 (t,  $J = 7.4$  Hz, 2H), 2.75 (t,  $J = 7.2$  Hz, 2H), 2.66 – 2.61 (m, 2H), 1.62 (p,  $J = 7.3$  Hz, 2H), 1.36 – 1.29 (m, 2H), 1.28 – 1.18 (m, 8H), 0.84 (t,  $J = 7.0$  Hz, 3H).  $^{13}\text{C}$  NMR (176 MHz,  $\text{DMSO-}d_6$ )  $\delta$  172.35, 162.41, 162.35, 130.44, 130.38, 126.22, 126.08, 125.96, 37.92, 36.07, 34.72, 31.93, 31.21, 28.57, 28.55, 28.48, 27.73, 22.07, 13.94. HRMS (ESI) calcd. for  $\text{C}_{27}\text{H}_{31}\text{N}_2\text{O}_6\text{S}_2$   $[\text{M}+\text{H}]^+$  543.1624; obs. 543.1626.



$^1\text{H}$ -NMR spectrum of compound 7.

$^{13}\text{C}$ -NMR spectrum of compound 7.





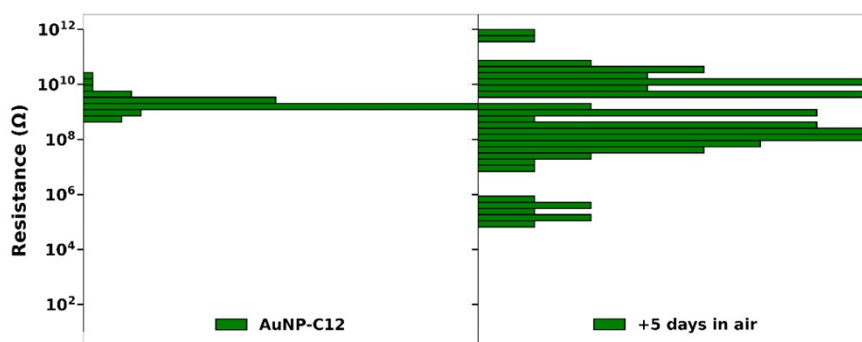
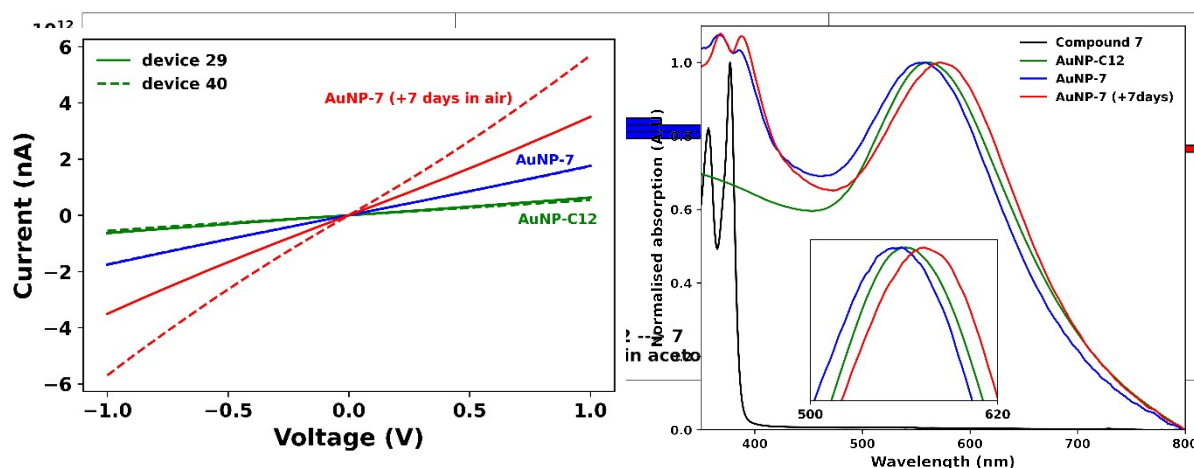


**Figure S12: Solid phase exchange of C12 with SS038**

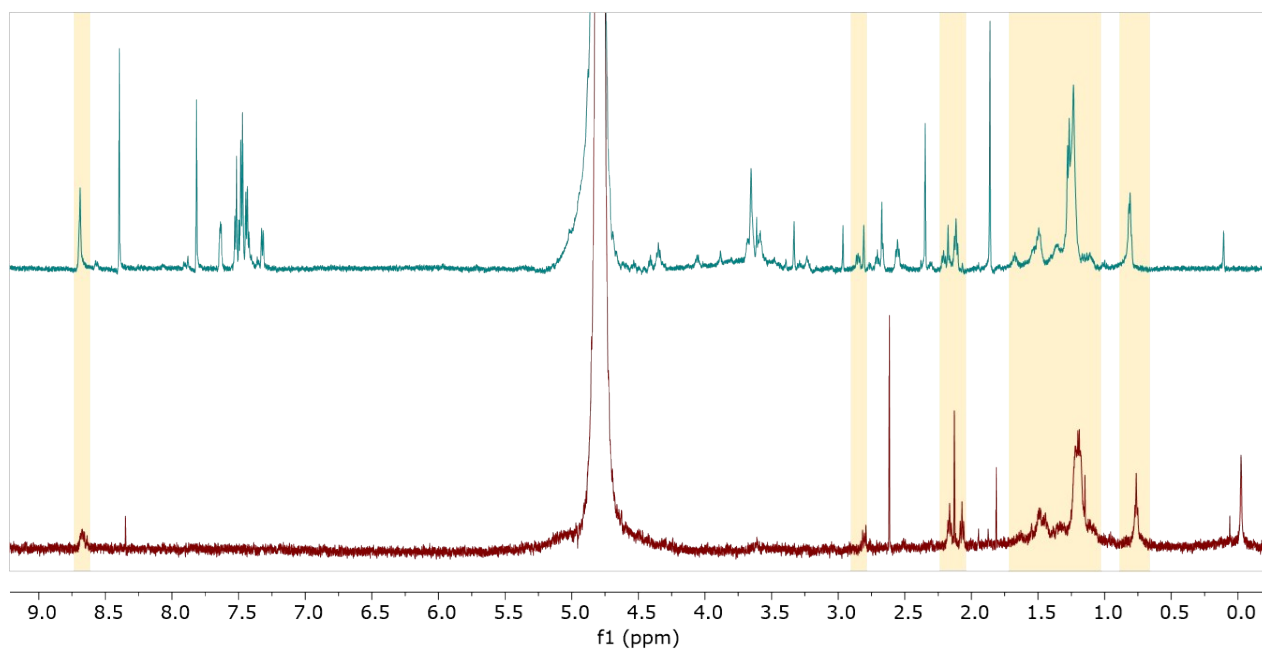
Resistance distribution of 80 devices covered by an AuNP-C12 monolayer cast on a convex water surface from a colloidal hexane-chloroform solution. After five days in air, the resistance of the devices span over multiple order of magnitude indicating degradation of the AuNP-C12 array.

A second AuNP-C12 array was deposited as above and showed a comparable resistance distribution. Upon immersion for four hours in 1mM of compound 7 in acetone, the average resistance of all devices decreased by a factor of two. Upon seven days in air, the average resistance of the devices remains identical or further decrease as compared to after ligand exchange. The UV-Vis spectroscopy of AuNP-C12 before and after exchange with SS038 show the signatures below 400 nm of SS038, confirming that C12 has been replaced by the NDI



molecule.

**Figure S13:  $^1\text{H-NMR}$  spectra of AuNP-7 (top) and 7 (bottom).**



It is noteworthy that the signal-to-noise ratio is lower for **7**, due to its limited solubility in D<sub>2</sub>O. The signals present in both spectra have been highlighted.

## References

1. Wang, Y.; Liu, D.; Zheng, Q.; Zhao, Q.; Zhang, H.; Ma, Y.; Fallon, J. K.; Fu, Q.; Haynes, M. T.; Lin, G.; Zhang, R.; Wang, D.; Yang, X.; Zhao, L.; He, Z.; Liu, F., Disulfide Bond Bridge Insertion Turns Hydrophobic Anticancer Prodrugs into Self-Assembled Nanomedicines. *Nano Letters* **2014**, *14* (10), 5577-5583.
2. Cheng, J.; Miller, C. J., Quantum Interference Effects in Self-Assembled Asymmetric Disulfide Monolayers: Comparisons between Experiment and ab Initio/Monte Carlo Theories. *The Journal of Physical Chemistry B* **1997**, *101* (6), 1058-1062.
3. Nuhn, L.; Braun, L.; Overhoff, I.; Kelsch, A.; Schaeffel, D.; Koynov, K.; Zentel, R., Degradable Cationic Nanohydrogel Particles for Stimuli-Responsive Release of siRNA. *Macromolecular Rapid Communications* **2014**, *35* (24), 2057-2064.